Available online at www.sciencedirect.com

SciVerse ScienceDirect

Ceramics International 38 (2012) 1655–1661

CERAMICS INTERNATIONAL

www.elsevier.com/locate/ceramint

Nanocrystalline AMn_2O_4 (A = Co, Ni, Cu) spinels for remediation of volatile organic compounds—synthesis, characterization and catalytic performance

S.A. Hosseini [a,*], A. Niaei [a], D. Salari [a,*], S.R. Nabavi [b]

[a] Department of Applied Chemistry and Chemical Engineering, Faculty of Chemistry, University of Tabriz, Tabriz, Iran
[b] Faculty of Chemistry, University of Mazandaran, Babolsar, Iran

Received 14 May 2011; received in revised form 3 September 2011; accepted 28 September 2011
Available online 15 October 2011

Abstract

Nanocrystalline AMn_2O_4 (A = Co, Ni, Cu) manganite spinels were prepared by using the sol–gel auto combustion method under the same synthesis conditions and their physico-chemical properties were studied by XRD, UV–vis DRS, SEM, BET and FTIR. Besides, the reducibility of oxides was studied by temperature-programmed reduction (TPR). The relationship between the properties and activity of spinels in oxidation of 2-propanol and toluene was investigated. Among all, nickel manganite exhibited the most promising activity, in which the completed conversion of 2-propanol and toluene occurred at 250 and 350 °C, respectively. Higher activity of nickel manganite oxide was explained in terms of the synergetic effect between Mn^{3+} and Ni^{2+} phases in nickel manganite oxide. No direct relationship was resulted between activity with either specific surface area or particle size of manganite oxides. No correlation was found between activity and energy band gap of the oxides. The study showed that the nickel manganite nano oxides could be promising catalysts for VOC removal. A relationship between VOC's structure and reactivity for conversion over catalysts was revealed, in which 2-propanol showed more reactivity than toluene to be converted over these catalysts.

Keywords: Manganite spinel; Catalytic combustion; Sol–gel; 2-Propanol; Energy band gap

1. Introduction

Volatile organic compounds (VOCs) have a high vapor pressure and low water solubility and are recognized either as major contributors of air pollution either, through their toxic nature, or as precursors of ozone and photochemical smog [1,2].

From an economical point of view, catalytic oxidation of VOCs is an interesting technology due to the energy saving features and minimization of the formation of by-products, such as dioxins and nitrogen oxides. Moreover, catalytic oxidation appears to be more efficient for the abatement of low concentrations of contaminant (<1000 ppm), which cannot be thermally combusted without additional fuel [3].

Driven by the necessity of decreasing manufacturing cost and increasing resistance to toxicity of commercial catalysts for volatile organic compounds (VOCs) elimination, efforts have been made to develop metal oxide catalysts, which can exhibit the activity similar or higher than that of noble metal catalysts [4]. Spinel type mixed oxides due to their high thermal resistance and specific catalytic and/or electronic properties are of importance. They are used in sensor and semiconductor technology as well as in heterogeneous catalysis [5,6].

There are some papers about the application of spinel-type oxides in remediation of volatile organic compounds. $CuCo_2O_4$ and $CoCr_2O_4$ spinels were found to be very active for CO and hydrocarbons oxidation, as well as for catalytic removal of NO_x and diesel soot [7–13]. It has been known that mixed oxides exhibit improved properties rather than individual oxides, especially in the environmental catalysis. These transition metals, especially manganese oxides are considered friendly environmental [14–17].

The objectives of this work were to synthesize several manganite oxides under the same preparation conditions and the study of their properties and activities to develop as friendly environmental catalysts in oxidation of VOCs. Herein, Co, Ni

* Corresponding authors. Tel.: +98 411 3393163, fax: +98 411 3340191.
E-mail addresses: s_ali_hosseini@yahoo.com (S.A. Hosseini), salari_dariush@yahoo.com (D. Salari).

0272-8842/$36.00
doi:10.1016/j.ceramint.2011.09.057

and Cu were chosen as A site cations for preparation of AMn_2O_4 because of their application in catalytic oxidation [1,18]. The spinels were synthesized by sol–gel auto combustion under the same conditions to obtain highly active catalysts [19]. Among methods used for synthesis of nano oxides, sol–gel combustion was preferred due to its advantages established in literature [20,21].

Sol–gel combustion method combines the advantages of sol–gel technique, such as obtaining pure-phase mixed oxides with a good control of stoichiometry and nanoparticle size, and combustion method enabling production of highly defective materials.

The activities of these catalysts are evaluated for volatile organic compounds different in essence. Toluene and 2-propanol were selected as models of VOCs, which are commonly used in chemical and petrochemical industries [1,22]. The catalysts were characterized by XRD, FTIR, SEM, BET, UV–vis DRS and TPR.

2. Materials and methods

2.1. Catalyst synthesis

All materials used for the synthesis of spinels were supplied by Merck Company. The catalysts were prepared by sol–gel auto combustion method as described in our previous papers [20,21]. The initial reactant mixtures contained aqueous solutions of Mn, Co, Ni, and Cu nitrates. The molar ratios of Cu, Co and Ni to manganese were 1:2 and stoichiometric amount of citric acid monohydrate as fuel to total nitrate moles was kept to be 0.4. The homogeneously mixed solution was placed in a 2 L beaker, heated up to 60 °C and continuously stirred by using a magnetic agitator for several hours to remove the excess of water. Then, the solutions were heated up to about 80 °C and stirred constantly, transforms into a sticky gel. Slow heating the gel up to 180 °C results in auto-combustion process with a formation of a black fluffy material. The reaction is noticeably exothermic, which leads to a thermal peak above 1000 °C in the reacting solid mixture for a few seconds. The samples were then calcined at 700 °C for 6 h to ensure the absence of carbonaceous residues, which may remain in the samples.

2.2. Catalyst characterization

X-ray diffraction (XRD) studies were carried out on a SIEMENS D5000 diffractometer, equipped with Kristalloflex 760 X-ray generator and with a curved graphite monochromator which made the selection of the Cu K radiation (40 kV/30 mA) possible. Measurements of the samples were carried out in the range 2θ of 16–67°, at a scanning rate of 1°/min.

For FTIR spectroscopy, the samples were pressed into self-supporting wafers of 10–15 mg/cm^2 surface density and placed into a glass cell sealed by KBr windows. The spectra were recorded in transmittance at room temperature using a Bruker spectrometer (model TENSOR 27).

UV–vis diffuse reflectance spectra were recorded at 27 °C in the wavelength range of 250–900 nm using a Scinco210 spectrophotometer (model AA-1301) equipped with an integral sphere. The powdered sample was placed in a reflectance cell made of fused silica that is capable of in situ measurements after evacuation of the sample at higher temperatures. Spectralon (Labsphere, USA) was used as the reference material.

The BET surface area and pore volume of the prepared catalysts were determined by means of N_2 isotherms measured at −196 °C by using a micro pore analyzer (ASAP 2010, USA). The shape and size of the synthesized particles were determined via scanning electron microscopy (SEM) by EQ-C1-1 instrument through pre-coating samples with gold.

Temperature-programmed reduction (TPR) measurements were carried out with Micrometritics Autochem 2910. Catalyst samples were pre-treated with a mixture of 5 vol.% oxygen in helium at 500 °C for 2 h. Hydrogen consumption was measured with a flow of mixture of 5 vol.% H_2 in argon at 20 cm^3/min and a linear heating rate of 10 °C/min in the 50–950 °C range.

2.3. Evaluation of catalytic performance

The VOCs combustion reactions were carried out in a tubular (i.d. = 8 mm) fixed bed pyrex glass reactor at atmospheric pressure and different temperatures in an electrical furnace controlled by a proportional–integral–derivative controller (PID). Catalyst (0.2 g) was placed over a plug of glass wool and a thermocouple was embedded inside the catalyst bed. Before starting each run, catalysts were pre-treated with 10 mL/min of pure nitrogen at 400 °C for 40 min in order to eliminate the possible compounds adsorbed on the catalyst surface. After this pretreatment, the reactor was cooled at 100 °C, and the reaction vapor was introduced by passing the carrier gas (nitrogen) flow through a saturator containing 2-propanol and toluene mean while air stream was used to maintain the molar concentration of 2-propanol and toluene, which is about 0.2% in the full stream. All experimental runs were taken under steady state conditions. More details about the experimental set up have been presented in [1].

The analyses of the products derived from the catalytic activity measurement were carried out in a Shimadzu 2010 gas chromatograph apparatus with a flame inductivity detector (FID) and CBP20 capillary column.

In order to meet the requirement of adsorption at infinite dilution, corresponding to zero coverage and GC linearity, injected amounts were about 1 μL. Air was used as a marker for the retention time correction, and it was used to ensure the absence of dead volume when a new column was placed in the chromatograph.

3. Results and discussion

The results of X-ray diffraction analyses confirmed the formation of a spinel structure in all the catalysts, but some impurity of metal oxides (CuO, NiO) and reverse spinel $MnCo_2O_4$ (10 wt.%) were observed in the synthesized samples

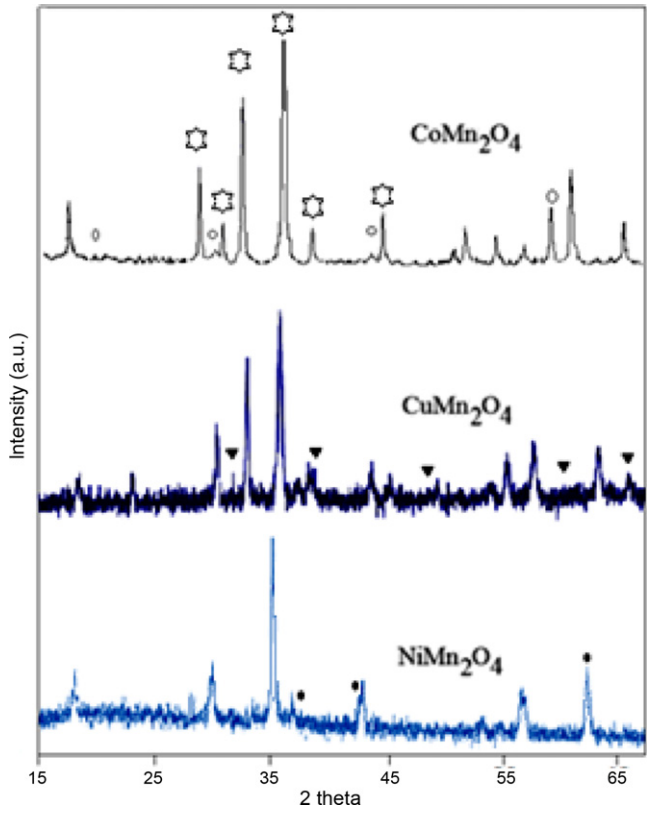

Fig. 1. XRD pattern of AMn_2O_4 (A = Co, Ni, Cu). $CoMn_2O_4$ (☆), $MnCO_2O_4$ (○), CuO (▼) and NiO (●).

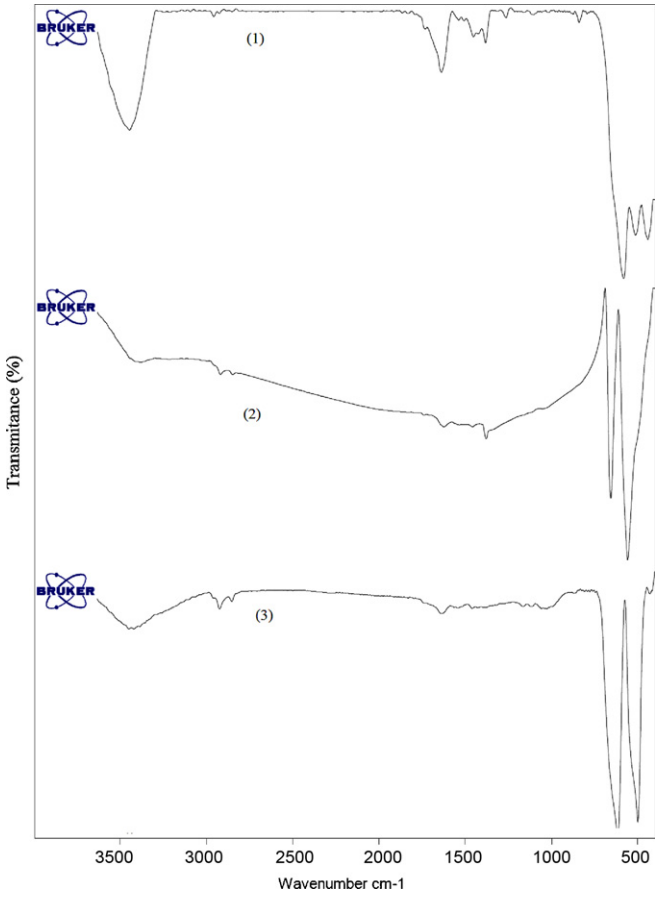

Fig. 2. FTIR spectra of $NiMn_2O_4$ (1), $CuMn_2O_4$ (2) and $CoMn_2O_4$ (3).

(Fig. 1). In the XRD pattern of $NiMn_2O_4$, the peaks in $2\theta = 37.5$, 43, 62.5 are ascribed to the presence of NiO phase (JCPDS 47-1049), whereas CuO peaks in $CuMn_2O_4$ pattern were observed at $2\theta = 35.25$, 38.5, 48.63, 61.40, 67.91 according to JCPDS 44-0706. The appearance of peaks at $2\theta = 18.7$, 31, 36, 44, 58 revealed the presence of reverse spinel of $MnCo_2O_4$ in the sample. $NiMn_2O_4$ showed a cubic spinel structure in contrast to other manganites, i.e. MMn_2O_4 (Co, Cu), showing a tetrahedral structure. Furthermore, through the sharpest peak of XRD patterns (around 36°), the mean crystallite size of the oxides was estimated using Scherer formula [1]. The calculated crystallite sizes for $NiMn_2O_4$, $CuMn_2O_4$, and $CoMn_2O_4$ were 15, 13 and 10 nm, respectively.

Another proof to confirm the existence of the spinel structure in these samples is FTIR results. Spinel type oxides exhibit two distinguished bands in wave number range between 400 and 700 cm^{-1}[23], therefore in order to confirm the formation of spinel structure, FTIR analyses were carried out (Fig. 2). For all samples two peaks are observed in this wave number range. The bands above 580 cm^{-1} correspond to vibration of atoms in tetrahedral oxygen environment (A–O at AMn_2O_4) in spinels, while the bands around 517, 499.49 and 561.18 cm^{-1} correspond to vibration of atoms in the octahedral oxygen environment (mainly manganese) in $NiMn_2O_4$, $CoMn_2O_4$ and $CuMn_2O_4$, respectively. The bands at 444.85 and 432.35 cm^{-1} indicate the vibration mode of Ni–O–Mn and Co–O–Mn in $NiMn_2O_4$ and $CoMn_2O_4$, respectively. The broader peaks for $NiMn_2O_4$ and $CuMn_2O_4$ versus to $CoMn_2O_4$ indicate that these samples contain a broader distribution of metal cation type and cation oxidation states in both tetrahedral and octahedral sites [18]. The results of FTIR are in agreement with XRD results about distribution of oxides in samples in the form of spinel mixed oxides and single oxides. The broad peak around 3500 cm^{-1} is ascribed to chemisorbed water. Compared to FTIR bands of bulk materials, there is a shift in IR active mode, which is due to nano size grains [26]. For a nano size grain, the atomic arrangements on the boundaries differ greatly from that of bulk crystals both in co-ordination number and bond lengths, showing some extent of disorder [24]. Crystal symmetry is thus, degraded in nano size grains. The degradation in crystal symmetry results in the shifting of IR active mode [25,26]. Fig. 3 shows the morphology and particle size distribution of manganite spinels. The morphology of catalysts is similar in shape, which is as grain. The mean particle size of $CoMn_2O_4$, $CuMn_2O_4$, and $NiMn_2O_4$ are round 35, 40 and 50 nm, respectively. The related BET surface areas are 31, 29.4, and

Table 1
BET surface area and particle sizes of samples.

Catalyst name	Specific surface area (m^2/g)	Mean particle size (nm)
$NiMn_2O_4$	27.2	50
$CuMn_2O_4$	29.4	40
$CoMn_2O_4$	31	35

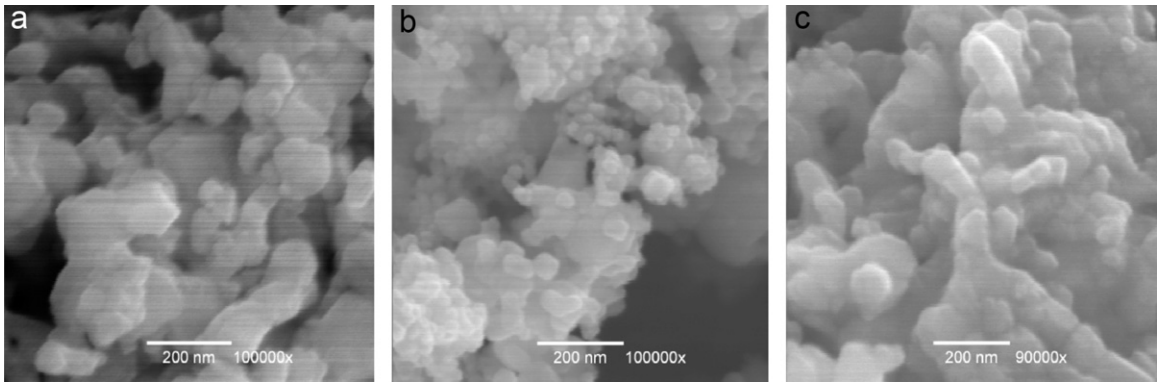

Fig. 3. SEM micrographs of manganite spinels: $NiMn_2O_4$ (a), $CuMn_2O_4$ (b), and $CoMn_2O_4$ (c).

27.2 m^2/g, respectively (Table 1). As we expected there is a reverse relationship between particle size and specific surface area of samples.

Fig. 4 presents the UV–vis diffuse reflective spectra of spinels. In the case of all spectra, an absorption band is observed around 316 nm, which corresponds to the excitation of surface plasmons in the composite nanoparticles. In the case of spectrum of $CoMn_2O_4$, another strong band is observed at 550 nm ascribed to the excitation of surface plasmons [27]. In addition to these bands, some additional absorption bands are observed at wavelengths above 760 nm. These bands may be due to coupling of the plasmon modes between neighboring particles [27]. It is observed in Fig. 4 that absorption decreases with the increase in wavelength.

Energy band gap (E_g) of samples was determined through UV–vis spectra.

Energy band gap of material is related to absorption coefficient α by the Tauc relation [27,28].

$$ahv = A(hv - E_g)^n \quad (1)$$

where A is a constant, $h\nu$ the photon energy, E_g the band gap and n is an index which assumes values 1/2, 3/2, 2 or 3 depending on the nature of the electronic transition responsible for the absorption. $n = 1/2$ is taken for an allowed direct transition. Therefore, by plotting a graph between $(\alpha h\nu)^2$ and $h\nu$ in eV, a straight line is obtained, giving the value of the direct band gap. The band gaps calculated for $NiMn_2O_4$, $CuMn_2O_4$, and $CoMn_2O_4$ were 1.543, 1.58 and 1.536 eV, respectively.

In order to investigate the reducibility of the series of catalysts, H_2-TPR experiments were carried out and the results are shown in Fig. 5. In the case of TPR curve for $CuMn_2O_4$, a peak was appeared around 229 °C, indicating the reduction of Cu^{2+} to metallic copper. For TPR curves of $CoMn_2O_4$ and $NiMn_2O_4$ the peaks around 380–430 °C are due to the reduction of Mn_2O_3 to Mn_3O_4 and the reduction of Mn_2O_3 to Mn_3O_4, respectively. The TPR curve for reduction of Mn_2O_3 is shown in Fig. 5. Mn_2O_3 exhibited two reduction peaks including reduction of Mn_2O_3 to Mn_3O_4 as well as Mn_3O_4 to MnO. Appearance of peak around 480–500 °C for $CoMn_2O_4$ is because of transformation of Mn_3O_4 to MnO [18].

In TPR curve of $CoMn_2O_4$, the reduction peak around 670 °C is due to reduction of Co^{2+} into metallic cobalt [20], whereas reduction peak of Ni^{2+} to metallic nickel happens around 680 °C. The activities of spinels were evaluated in catalytic combustion of 2-propanol and toluene.

Fig. 6 shows the catalytic performances of the manganites in combustion of 2-propanol. It is observed that $NiMn_2O_4$ exhibited the higher activity than others in combustion of 2-propanol, and the order of activity of catalysts was as followed:

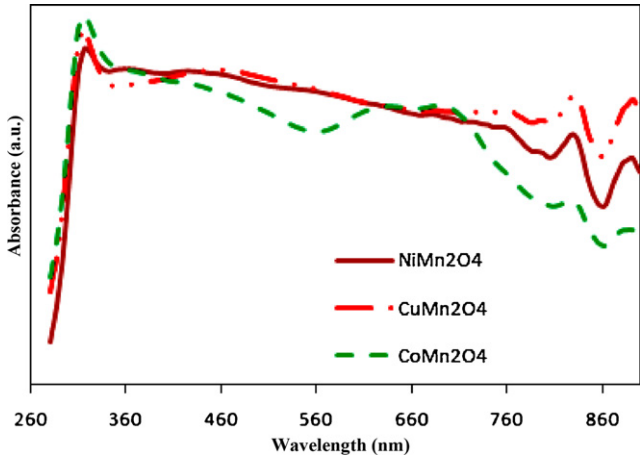

Fig. 4. UV–vis diffuse reflective spectra of spinel-type manganites.

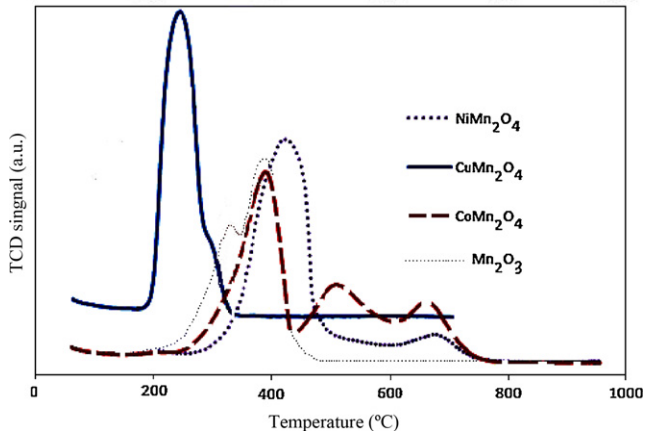

Fig. 5. TPR curves for AMn_2O_4 (A = Co, Ni and Cu) and Mn_2O_3 catalysts.

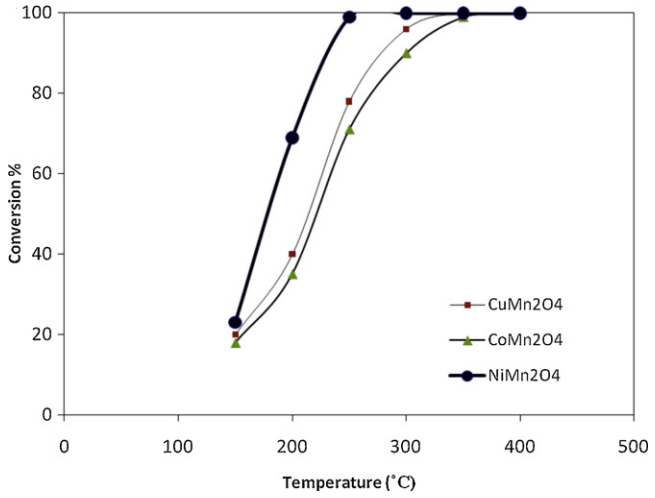

Fig. 6. Light-off curves for conversion of 2-propanol over spinel catalysts.

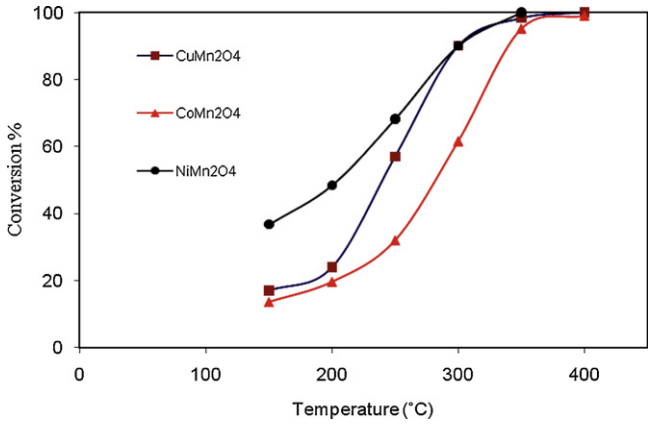

Fig. 7. Light-off curves for conversion of toluene over spinel catalysts.

$NiMn_2O_4 > CuMn_2O_4 > CoMn_2O_4$. As confirmed by XRD results, quite a larger amount of NiO was formed during synthesis at the same preparation conditions.

Combining the results of XRD, FTIR and TPR with catalytic activity results, the higher activities of $NiMn_2O_4$ and $CuMn_2O_4$ versus $CoMn_2O_4$ are ascribed to presence of active sites of Mn^{3+}, Ni^{2+} and Cu^{2+} in former samples. The higher activity of nickel manganite oxide is ascribed to higher content of Mn^{3+} and the synergetic effect of between manganese in spinel and Ni^{2+} cations.

To investigate this matter, some Ni–Mn mixed oxides with different molar ratios of nickel and manganese were prepared, which were $NiMn_2O_4$, $Ni_{1.5}Mn_2O_x$, $Ni_{1.75}Mn_2O_x$, $Ni_2Mn_2O_x$, and Ni_2MnO_x and their activities were studied in combustion of 2-propanol and toluene. The results (not presented here) confirmed that the activity of mixed oxides enhanced with the increase of Ni content in the samples. $Ni_2Mn_2O_x$ showed the highest activity and for the activity of Ni_2MnO_x was lower than that of $Ni_2Mn_2O_x$.

The result is in agreement with results obtained by Tang et al. about oxidation of benzyl alcohol by using Mn–Ni mixed oxides [29]. They found that the synergistic interactions between Mn^{3+} and Ni^{2+} cations through oxygen bonding enhance the activity of Mn–Ni catalysts for benzyl alcohol oxidation and the activity of catalysts increased with the accretion of Ni content in catalysts. They resulted that the reducibility of mixed oxides shifted to lower temperature with the increase of Ni content in Ni–Mn oxides.

A similar trend for activity of catalyst was observed in the combustion of toluene over the catalysts (Fig. 7). The only difference was that the conversion became less because of lower reactivity of toluene rather than 2-propanol which is in agreement with our previously study [18]. The spinel mixed catalysts exhibit higher activity In comparison with single and bimetal catalysts [1,2,30].

The catalytic oxidation of organic compounds over metal oxides proceeds according to the Mars Van Krevelen mechanism [18,31], where the organic molecule is oxidized by the lattice oxygen of the oxide, the latter being re-oxidized by gas phase oxygen. It is an important condition for this mechanism to have metal couples in different oxidation states, which could be oxidized or reduced therefore the reaction would be realized [32]. Existence of more active sites increases the activity of catalysts. The presence of more active sites of Mn^{3+} and Ni^{2+} in $NiMn_2O_4$ could be one of the reasons for higher activity of $NiMn_2O_4$. Nevertheless, TPR results showed that those cited above are not the only causes responsible for the observed activity trends. Synergistic effect between Mn and Ni oxides is an influencing factor for higher activity of the catalyst.

By comparing the results of particle size and BET surface area with catalytic activities revealed that there is no direct relationship between the activity and either BET surface area or particle size. The $CoMn_2O_4$ with smaller particle size and higher specific surface area showed lower activity than $CuMn_2O_4$, revealing that expected particle size, specific surface area and other parameters affect the activity of catalysts. This result is in agreement with other researcher results [33,34].

In the case of oxidation mechanism of VOC, the activation of the weakest C–H bond is the rate determining step (slow step) for their oxidation despite the presence of a wide variety of functional groups in the substrates tested. For all organic compounds, bond strength seems to be a key parameter for determining reactivity of the compounds and the slow step is the cleavage, with the aid of catalyst surface, of the weakest C–H of the VOC. For the linear hydrocarbons, the reaction mechanism could be similar to that developed by Busca et al. [35,36] over metal oxides. For the cyclic and aromatic compounds (such as toluene), their C–H bonds are stronger than those of corresponding linear compounds, but the species coming from their adsorption on the surface catalyst are thermodynamically less stable, so the temperatures required for their conversion are less important. For the oxygenated compounds, there is no simple linear dependence between C–H bond strength and $T_{50\%}$. This result indicates that the C–H bond strength is not the only factor determining the conversion temperature. The mechanistic process during catalytic oxidation is more complex, taking into account additional factors such as the presence of functional groups [37].

Besides other properties, we determined the energy band gap of these mixed oxides. Considering the energy band gap and activities of samples indicated that there is no the straight relationship between activity and energy band gap for these samples. The order of catalytic activities of spinels was as follows: $NiMn_2O_4 > CuMn_2O_4 > CoMn_2O_4$, whereas the order of energy band gaps was as $CuMn_2O_4 > NiMn_2O_4 > CoMn_2O_4$. $CoMn_2O_4$ with lowest E_g showed the lowest catalytic activity, whereas $NiMn_2O_4$ with middle E_g showed the highest activity. This means that energy band gap is not an influencing factor for activities of the manganite samples.

4. Conclusions

Spinel type nano oxides of AMn_2O_4 (A = Co, Ni and Cu) were successfully synthesized under the same conditions by using the sol–gel combustion method, and their activities were evaluated in the combustions of toluene and 2-propanol. The spinel structures of catalysts were confirmed by XRD and FTIR. No direct relationship was concluded between activity with either particle size or specific surface area of the manganite spinels.

The study revealed that synergistic effect among AO and spinel oxides and stability of active sites in reaction temperature indicated that these are effective factors on the activity of catalyst. The higher activity of nickel manganite oxide is attributed to the high synergetic effect between Mn and Ni on the oxide, containing the more active Ni^{2+} and Mn^{3+} sites. No direct relationship was concluded between energy band gap of manganite spinels and catalytic activity. Sol–gel auto combustion is a promising method for synthesis of nano oxides with high catalytic activity.

Acknowledgment

Especially thank Iranian Nanotechnology Initiative Council for financial supports.

References

[1] S.A. Hosseini, A. Niaei, D. Salari, A. Jodaei, Study of catalytic activities of nanostructure copper and cobalt supported ZSM-5 catalysts for conversion of volatile organic compounds, Turk. J. Chem. 34 (2010) 15–25.
[2] C. Hort, S. Gracy, V. Platel, L. Moynault, Evaluation of sewage sludge and yard waste compost as a biofilter media for the removal of ammonia and volatile organic sulfur compounds (VOSCs), Chem. Eng. J. 152 (2009) 44–53.
[3] D. Delimaris, T. Ioannides, VOC oxidation over CuO–CeO_2 catalysts prepared by a combustion method, Appl. Catal. B 89 (2009) 295–302.
[4] D. Delimaris, T. Ioannides, VOC oxidation over MnO_x–CeO_2 catalysts prepared by a combustion method, Appl. Catal. B 84 (2008) 303–312.
[5] M. Alifanti, M. Florea, V.I. Pârvulescu, Ceria-based oxides as supports for $LaCoO_3$ perovskite; catalysts for total oxidation of VOC, Appl. Catal. B 70 (2007) 400–405.
[6] B. Levasseur, S. Kaliaguine, Effects of iron and cerium in $La_{1-y}Ce_yCo_{1-x}Fe_xO_3$ perovskites as catalysts for VOC oxidation, Appl. Catal. B 88 (2009) 305–314.
[7] S.C. Kim, The catalytic oxidation of aromatic hydrocarbons over supported metal oxide, J. Hazard. Mater. B. 91 (2002) 285–299.
[8] J. Kirchnerova, D. Klvana, Design criteria for high-temperature combustion catalysts, Catal. Lett. 67 (2000) 175–181.
[9] P. Stefanov, I. Avramova, D. Stoichev, N. Radic, B. Grbic, Ts. Marinova, Characterization and catalytic activity of Cu–Co spinel thin films catalysts, Appl. Surf. Sci. 245 (2005) 65–72.
[10] D. Fino, N. Russo, G. Saracco, V. Specchia, CNG engines exhaust gas treatment via Pd-Spinel-type-oxide catalysts, Catal. Today 117 (2006) 559–563.
[11] U. Zavyalova, V.F. Tretyakov, T.N. Burdeynaya, V.V. Lunin, A.I. Titkov, A.N. Salanov, P.G. Tsyrulnikov, J. Petrol. Chem. 45 (4) (2005) 255–260.
[12] D. Fino, N. Russo, G. Saracco, V. Specchia, Catalytic removal of NO_x and diesel soot over nanostructured spinel-type oxides, J. Catal. 242 (2006) 38–47.
[13] H.G. El-Shobaky, Surface and catalytic properties of Co, Ni and Cu binary oxide systems, Appl. Catal. A 278 (2004) 1–9.
[14] W.B. Li, W.B. Chu, M. Zhuang, J. Hua, Catalytic oxidation of toluene on Mn-containing mixed oxides prepared in reverse microemulsions, Catal. Today 93-95 (2004) 205–209.
[15] V.P. Santos, M. Pereira, J.J. Orfeo, J. Figueiredo, The role of lattice oxygen on the activity of manganese oxides towards the oxidation of volatile organic compounds, Appl. Catal. B 99 (2010) 353–363.
[16] L. Markov, A. Lyubchova, Precursor control of the inversion degree of magnesium-cobalt spinels, J. Mater. Sci. Lett. 10 (1991) 512–514.
[17] J.B. Smith, T. Norby, Cation self-diffusion in $LaFeO_3$ measured by the solid state reaction method, Solid State Ionics 177 (2006) 639–646.
[18] S.A. Hosseini, D. Salari, A. Niaei, F. Deganello, G. Pantaleo, P. Hojati, Chemical-physical properties of spinel $CoMn_2O_4$ nano-powders and catalytic activity in the 2-propanol and toluene combustion: effect of the preparation method, J. Environ. Sci. Health A 46 (2011) 291–297.
[19] L. Castro, Synthesis and characterization of sol–gel Cu–ZrO_2 and Fe–ZrO_2 catalysts, J. Sol–Gel Sci. Technol. 25 (2002) 159–163.
[20] M. Morales, B.P. Barbero, L.E. Cadu's, Combustion of volatile organic compounds on manganese iron or nickel mixed oxide catalysts, Appl. Catal. B 74 (2007) 1–10.
[21] S.A. Hosseini, M. Sadeghi, A. Alemi, A. Niaei, D. Salari, L. Kafi, Synthesis, characterization, and performance of $LaZn_xFe_{1-x}O_3$ perovskite nanocatalysts for toluene combustion, Chin. J. Catal. 31 (2010) 747–750.
[22] A. Niaei, D. Salari, F. Aghazadeh, N. Çaylak, A. Sepehrianazar, Catalytic oxidation of 2-propanol over (Cr, Mn, Fe)–Pt/γ-Al_2O_3 bimetallic catalysts and modeling experimental results by artificial neural networks, J. Environ. Sci. Health A. 45 (2010) 454–463.
[23] A.V. Salker, S.M. Gurav, Electronic and catalytic studies on $Co_{1-x}Cu_xMn_2O_4$ for CO oxidation, J. Mater. Sci. 35 (2000) 4713–4719.
[24] J. Lu, Yang.F H., B. Kiu, G. Zou, Preparation, infrared spectroscopy, and phase stability of nanosized iron silicide powders, Mater. Res. Bull. 34 (1999) 2109.
[25] S. Kurien, S. Sebastian, J. Mathew, K.C. George, Structural and electrical properties of nano-sized magnesium aluminate, Indian J. Pure Appl. Phys. 42 (2004) 926–933.
[26] N. Tharayil, R. Raveendran, A. Vaidyan, P. Chithra, Optical, electrical and structural studies of nickel–cobalt oxide nanoparticles, Indian J. Pure Appl. Phys. 15 (2008) 489–496.
[27] V. Kumar, S. Sharma, T.P. Sharma, V. Singh, Band gap determination in thick films from reflectance measurements, Opt. Mater. 12 (1999) 115–119.
[28] T.P. Sharma, D. Patidar, N.S. Saxena, K. Sharma, Measurement of structural and optical band gaps of $Cd_{1-x}Zn_xS$ (x = 4 and 6) nanomaterials, Indian J. Pure Appl. Phys. 44 (2006) 125–128.
[29] Q. Tang, C. Wu, R. Qiao, Y. Chen, Y. Yang, Catalytic performance of Mn–Ni mixed oxides hydroxide catalysts in liquid-phase benzyl alcohol oxidation using molecular oxygen, Appl. Catal. 403 (2011) 136–141.
[30] A. Jodaei, D. Salari, A. Niaei, M. Khatamian, S.A. Hosseini, Oxidation of ethyl acetate by a high performance nanostructure (Ni, Mn)–Ag/ZSM-5 bimetallic catalysts and development of an artificial neural networks predictive modeling, J. Environ. Sci. Health A 46 (2011) 50–62.
[31] Z. Abdullah, M. Bakar, S. Bhatia, A kinetic study of catalytic combustion of ethyl acetate and benzene in air stream over Cr-HZSM-5 catalyst, Ind. Eng. Chem. Res. 42 (2003) 6059–6067.
[32] I. Spasova, G. Ivanov, V. Georgescu, D. Mehandjiev, Complete oxidation of methyl–ethyl ketone and toluene over supported copper–chromium and

cobalt–chromium oxide catalysts, J. Univ. Chem. Technol. Metal. 41 (2006) 225–228.
[33] D.C. Kim, S.K. Ihm, Application of spinel-type cobalt chromite as novel catalyst for combustion of chlorinated organic pollutants, Environ. Sci. Technol. 35 (2001) 222–226.
[34] S.C. Kim, W.G. Shim, The effect of CeO_2 on the surface and catalytic properties of Pt/CeO_2–ZrO_2 catalysts for methane dry reforming, Appl. Catal. B 79 (2008) 149–156.
[35] M. Baldi, E. Finocchio, F. Milella, G. Busca, Catalytic combustion of C_3 hydrocarbons and oxygenates over Mn_3O_4, Appl. Catal. B 16 (1998) 43–51.
[36] G. Busca, E. Finocchio, G. Ramis, G. Ricchiardi, On the role of acidity in catalytic oxidation, Catal. Today 32 (1996) 133–143.
[37] V. Blasin-Aubé, J. Belkouch, L. Monceaux, General study of catalytic oxidation of various VOCs over $La_{0.8}Sr_{0.2}MnO_{3+x}$ perovskite catalyst—influence of mixture, Appl. Catal. 43 (2003) 175–186.